AIP | Advances

Excitation of surface waves on one-dimensional solid–fluid phononic crystals and the beam displacement effect

Rayisa P. Moiseyenko, Jingfei Liu, Sarah Benchabane, Nico F. Declercq, and Vincent Laude

Citation: AIP Advances **4**, 124202 (2014); doi: 10.1063/1.4903778
View online: http://dx.doi.org/10.1063/1.4903778
View Table of Contents: http://scitation.aip.org/content/aip/journal/adva/4/12?ver=pdfcov
Published by the AIP Publishing

Excitation of surface waves on one-dimensional solid–fluid phononic crystals and the beam displacement effect

Rayisa P. Moiseyenko,[1,2,a] Jingfei Liu,[2] Sarah Benchabane,[1]
Nico F. Declercq,[2] and Vincent Laude[1]
[1]*Institut FEMTO-ST, Université de Franche-Comté and CNRS, 15 B avenue des Montboucons, F-25030 Besançon Cedex, France*
[2]*Georgia Institute of Technology, UMI Georgia Tech – CNRS, George W. Woodruff School of Mechanical Engineering, Georgia Tech Lorraine, 2 rue Marconi, 57070 Metz-Technopole, France*

(Received 15 September 2014; accepted 26 November 2014; published online 5 December 2014)

The possibility of surface wave generation by diffraction of pressure waves on deeply corrugated one-dimensional phononic crystal gratings is studied both theoretically and experimentally. Generation of leaky surface waves, indeed, is generally invoked in the explanation of the beam displacement effect that can be observed upon reflection on a shallow grating of an acoustic beam of finite width. True surface waves of the grating, however, have a dispersion that lies below the sound cone in water. They thus cannot satisfy the phase-matching condition for diffraction from plane waves of infinite extent incident from water. Diffraction measurements indicate that deeply corrugated one-dimensional phononic crystal gratings defined in a silicon wafer are very efficient diffraction gratings. They also confirm that all propagating waves detected in water follow the grating law. Numerical simulations however reveal that in the sub-diffraction regime, acoustic energy of a beam of finite extent can be transferred to elastic waves guided at the surface of the grating. Their leakage to the specular direction along the grating surface explains the apparent beam displacement effect. [http://dx.doi.org/10.1063/1.4903778]

I. INTRODUCTION

The propagation of elastic waves at the surface of phononic crystals in air has attracted a lot of attention, due to potential applications in, *e.g.*, radio-frequency signal processing, sensing, and non-destructive evaluation.[1–6] Recently, surface waves propagating on periodically corrugated surfaces have been proposed to improve the acoustic beams emitted in fluids by transducers.[7,8] Indeed, when a phononic crystal is immersed in water, the dispersion of surface waves becomes strongly dependent on the coupling between acoustic (pressure) waves in the fluid and elastic waves in the solid parts. In this regard, the dispersion of surface waves has been studied for two-dimensional solid-solid phononic crystal plates immersed in water[9] and for deeply corrugated one-dimensional solid-fluid interfaces.[10] The excitation of surface waves at a solid-fluid interface from plane acoustic waves impinging from the fluid side is not always allowed. It is for instance forbidden if the dispersion relation of the surface wave lies below the sound cone, i.e., if its phase velocity is lower than the celerity of waves in the fluid, as in the case of the Scholte-Stoneley wave (SSW)[11,12] propagating at a planar and smooth solid/fluid boundary. Nevertheless, the excitation of surface waves from the solid side is in principle possible by means of the laser-induced thermoelastic effect,[13] by laser-ultrasonic spectroscopy or impulsive stimulated thermal scattering,[14,15] or by attaching piezoelectric elements

[a]Present address: Institut d'Electronique de Microélectronique et de Nanotechnologie, Cité Scientifique, 59652 Villeneuve d'Ascq Cedex, France

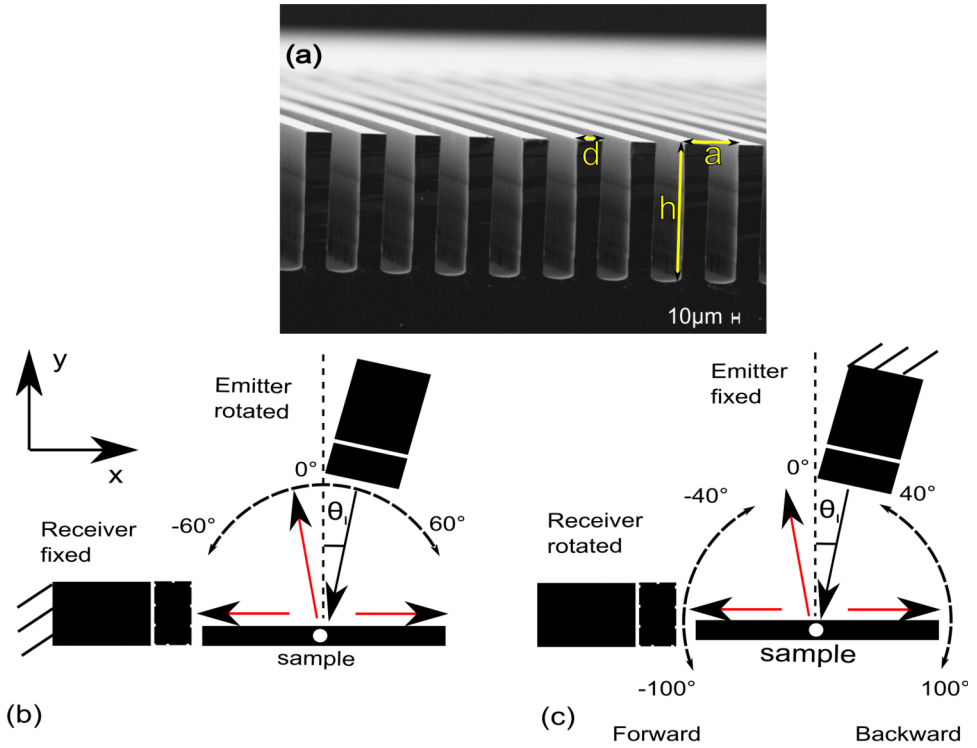

FIG. 1. Experimental set-up. (a) Two solid-fluid phononic crystals were fabricated in a silicon wafer by deep vertical deep etching through an optical lithography mask. The corrugation period is a = 100 μm and the groove width is d = 50 μm. The groove depth is h = 30 μm for sample A and 200 μm for sample B. A scanning electron microscope (SEM) image of sample B is shown. Diffraction measurements are performed with either (b) a varying angle of incidence and a fixed receiver or (c) a fixed angle of incidence and a rotating receiver. In the former case, the two possible receiver positions on either side of the sample are denoted as forward and backward, respectively.

directly to the phononic crystal. Surface waves can alternatively be generated through diffraction of plane acoustic waves by a periodic grating, as periodicity can provide the additional reciprocal lattice wave vector necessary to satisfy the matching of wavevectors projected along the interface. The diffraction of bulk acoustic waves on phononic crystals has been investigated recently,[16,17] though not in relation to the problem of exciting surface waves.[9,18]

It is rather easy to show that true, *i.e.*, non leaky, surface waves attached to a periodic solid-fluid interface cannot be excited by diffraction of a plane wave incident from the fluid, if diffraction results from the periodicity of the interface.[9] This theoretical result for infinitely extended plane waves is apparently contradicted by the experimental existence of the ultrasonic beam displacement effect. This interesting phenomenon appears for bounded beams incident on a corrugated interface in the sub-diffraction regime. It was predicted initially in the optical theory of gratings. Tamir and Bertoni pointed out that if the interface has a superimposed periodic structure, it is possible to cause a leaky wave to propagate in the backward direction, forcing a shift of the reflected beam.[19] The first experimental demonstration by Breazeale was in the ultrasonic domain using a shallow 1D corrugated brass grating immersed in water.[20] Optical positive and negative beam displacements were later observed when surface plasmon resonances or guided modes are excited.[21,22] In acoustics, surface waves, SSW and leaky Rayleigh waves were all mentioned as the reason for the beam displacement on shallow 1D corrugated gratings in water.[20,23–26] Reciprocally, the occurrence of a beam displacement can give a hint that guided modes have been excited.

In this paper, we investigate the possibility of surface wave generation by diffraction of pressure waves on deeply corrugated one-dimensional phononic crystal gratings.[10] Diffraction measurements with medium and deeply corrugated arrays of rectangular grooves defined in a silicon wafer confirm that all propagating waves detected in water follow the grating law, and thus do not reveal the

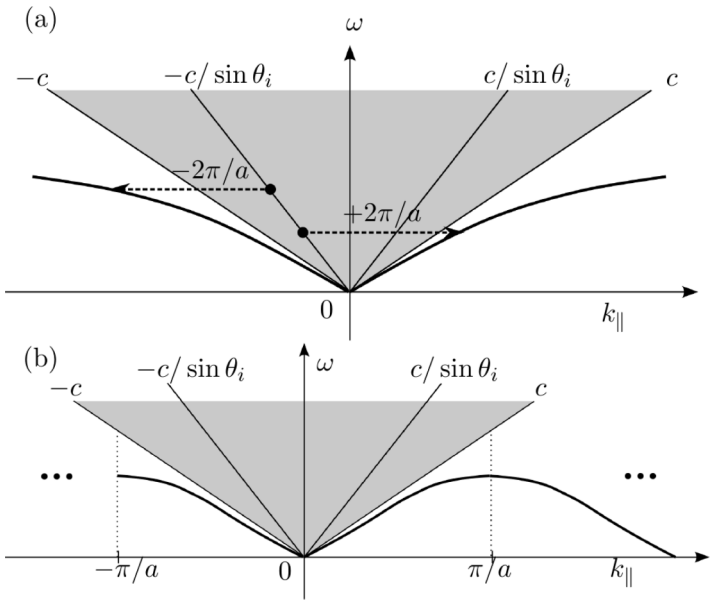

FIG. 2. Schematic representation of surface guided wave dispersion and excitation from the diffraction of bulk acoustic waves. (a) Possible diffraction processes from an incident plane bulk acoustic wave with angle of incidence θ_i to a surface mode whose dispersion lies below the sound cone. Phase-matching in the diffraction process involves a change in the wavenumber that is a multiple of $2\pi/a$, with a the lattice constant of the coupling phononic crystal grating. (b) Impossibility of the same diffraction process when the surface wave dispersion arises from the periodicity of the coupling grating: the edges of the first Brillouin zone are reached for $k = \pm\pi/a$, at which points folding of the surface wave dispersion bands occurs.

generation of surface waves. Further numerical simulations, however, show that the acoustic energy of a beam of finite extent can be partially transferred to the elastic waves of the grating. This transfer is especially efficient in the sub-diffraction regime, and occurs at discrete frequencies that can be associated with surface waves of the one-dimensional phononic crystal. Their leakage to the specular direction along the grating surface is very strong and explains the apparent beam displacement effect in the forward direction.

II. EXPERIMENTS

A. Experimental set-up

One-dimensional phononic crystal samples were prepared using microfabrication techniques into 500-micron thick silicon wafers, as shown in figure 1(a). The surface corrugation is defined by a mask that is transferred into a resist layer by UV lithography. Silicon is then deep-etched in a reactive ion etching machine. The aspect ratio of the etched grooves is better than 20, meaning that the walls of the corrugation are vertical to within 1°. Deep gratings are thus obtained, allowing us to enter the regime $h/a > 1$ where several surface waves can be present, with h the groove depth and a the lattice constant.[10] We selected a lattice constant $a = 100$ μm and a groove width $d = 50$ μm. Two different samples were prepared, with a groove depth $h = 30$ μm (sample A, $h/a = 0.3$) and $h = 200$ μm (sample B, $h/a = 2$).

Diffraction measurements were preformed using a polar C-scan system. The measured sample was immersed in a tank filled with water. A pair of transducers with nominal central frequency 15 MHz and wide emission bandwidth was used for the measurements. The emission beam width is about 10 mm, or 100 wavelengths, at 15 MHz in water. Diffraction measurements consist in the collection of time-waveforms taken at different diffraction angles or at different angles of incidence. The relative angular resolution for scans obtained using pulsed ultrasound is 0.1° under our experimental conditions. Experimental data are presented as angular spectrograms in the following.

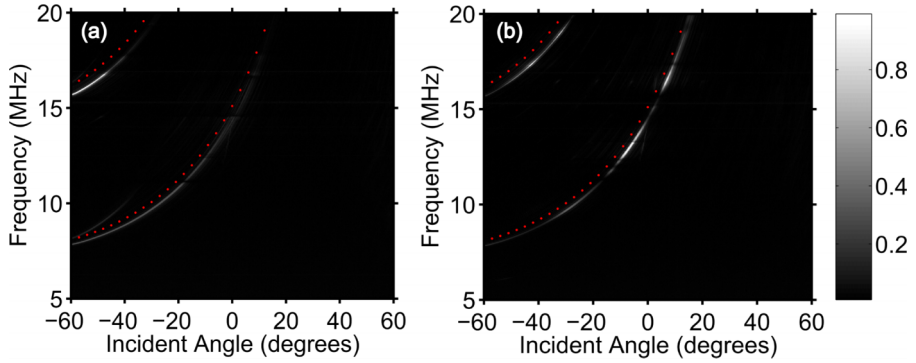

FIG. 3. Experimental spectrograms obtained with the grazing angle receiver / rotated emitter setup, (a) for sample A ($h/a = 0.3$) and (b) for sample B ($h/a = 2$). The gray scale is for the normalized spectrum of the electrical signal delivered by the receiver. The grating law (5) for the first two orders of diffraction is indicated with red dots.

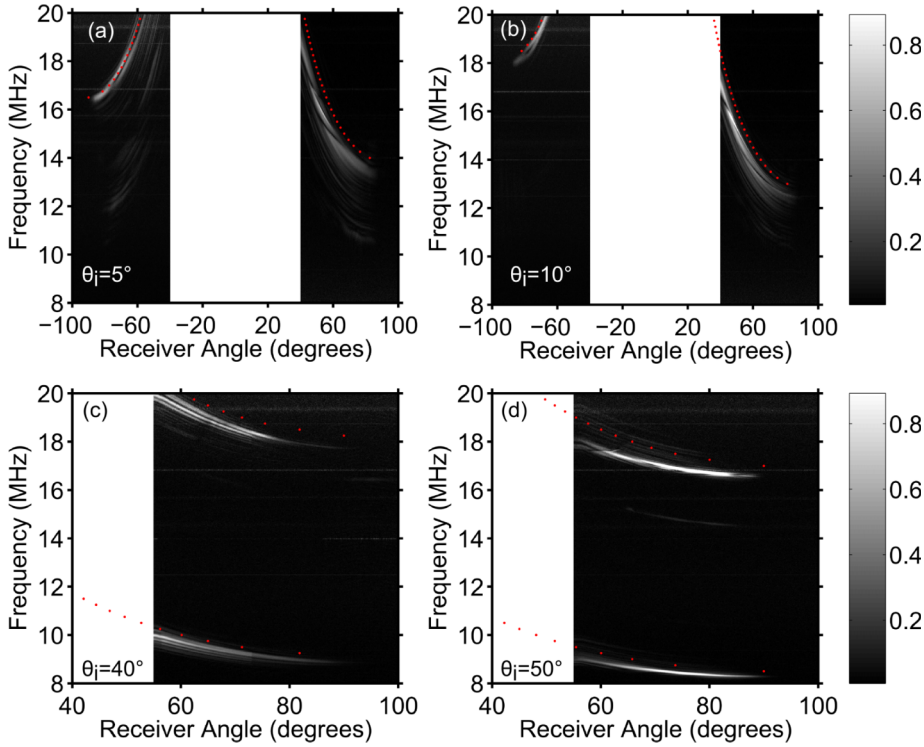

FIG. 4. Oblique incidence measurements for phononic crystal sample A ($h/a = 0.3$), obtained with the fixed emitter / rotated receiver setup. The red dotted line shows to the grating law (2). The incidence angle θ_i assumes the values (a) 5°, (b) 10°, (c) 40°, and (d) 50°.

The measurements have been performed in the two different configurations shown in figure 1. In the first one, depicted in figure 1(b), the receiver is fixed near one side of the sample and the emitter is rotated in order to vary the angle of incidence in the range $\theta_i = -60° \cdots 60°$. This way, we intend to record the appearance of orders of diffraction near the grazing angle, but also to record any signal that could be connected to the existence of a surface wave reaching the end of the sample surface. In the second configuration, depicted in figure 1(c), the emitter is fixed and the receiver is rotated. With this configuration, a complete picture of diffracted orders can be obtained.[16] Overall, with these two experimental arrangements, we can in principle record extensive information regarding propagating waves diffracted in water. Elastic waves excited in the phononic crystal sample, however, are not experimentally accessed.

B. Phase-matching conditions

Let us further precise the conditions for bulk and surface wave excitation by diffraction at the boundary between the phononic crystal and water. The grating law for plane waves imposes that the diffracted wavevector projected along the interface satisfies

$$k_{\parallel} = k_i + n\frac{2\pi}{a}, \tag{1}$$

with $k_i = -\sin\theta_i\omega/c$, where θ_i is the angle of incidence, ω is the angular frequency, and c is the celerity of waves in water ($c = 1480$ m/s). The minus sign results from the definition for angles in figure 1. The integer n is the order of diffraction. As pressure waves, diffracted bulk waves must satisfy the dispersion relation in water, $|k| = \omega/c$, resulting in the usual plane wave diffraction formula

$$\frac{\omega}{c}(\sin\theta_n + \sin\theta_i) = n\frac{2\pi}{a}, \tag{2}$$

with θ_n the propagation angle of the n-th order of diffraction and $k_{\parallel} = \sin\theta_n\omega/c$.

In contrast with bulk acoustic waves, surface guided waves combine a pressure distribution with a displacement distribution in the solid, and obey some dispersion relation $k_s(\omega)$. Note that the surface velocity $c_s(\omega) = \omega/k_s(\omega)$ is generally dispersive. Depending on the depth of the grooves, a number of modes exist for the one-dimensional solid-fluid phononic crystal.[10] A surface wave can in principle be excited if $k_{\parallel} = k_s(\omega)$ is satisfied for some frequency.[20] From the grating law, we find two different configurations where this relation can be satisfied, either backward diffraction given by

$$\omega(1/c_s(\omega) + \sin\theta_i/c) = n\frac{2\pi}{a}, n > 1, \tag{3}$$

or forward diffraction given by

$$\omega(1/c_s(\omega) - \sin\theta_i/c) = n\frac{2\pi}{a}, n > 1. \tag{4}$$

Backward and forward here refers to the surface wave traveling in the direction opposite to the incident bulk wave or in the same direction. For a given lattice constant a, imposed by the sample under consideration, the experimental parameters are the angle of incidence and the angular frequency. The overall situation is depicted in figure 2(a), for the general case of a surface guided wave. The incident plane wave is constrained to the sound cone for water, or condition $\omega/k_{\parallel} \geq c$. Surface guided waves exist under the sound cone and could not be excited without the help of diffraction. Generation of surface waves according to this principle is similar to an Umklapp process for phonons in crystal lattices.

The above discussion, however, does not take into account the fact that the periodic interface allowing for diffraction is also the locus of propagation of the surface guided wave. For the one-dimensional solid-fluid phononic crystal, the dispersion relation is influenced by periodicity and can be restricted to the first Brillouin zone, as depicted in figure 2(b). At the edges of the first Brillouin zone, for $k_s(\omega)a/(2\pi) = \pm 1/2$, the slope of the dispersion relation vanishes (the group velocity is zero). More significantly, the backward and forward diffraction conditions can never be achieved, since the required reciprocal lattice shift, $2\pi/a$, is also the width of the first Brillouin zone. According to this view, excitation of true surface guided waves from incident plane bulk acoustic waves is strictly forbidden. It remains, however, that leaky surface waves whose dispersion lies inside the sound cone can still in principle be excited. Leaky surface waves suffer of course from attenuation since they naturally couple to the continuum of acoustic waves in water. In the case of a bounded beam, in addition, the wavenumber is not strictly imposed by the dispersion relation, but for each frequency there is rather a distribution of wavenumbers given in a first approximation by the Fourier transform of the beam aperture. This remark implies that the excitation of a true surface wave is not precluded with a bounded beam, though its efficiency might still be limited.

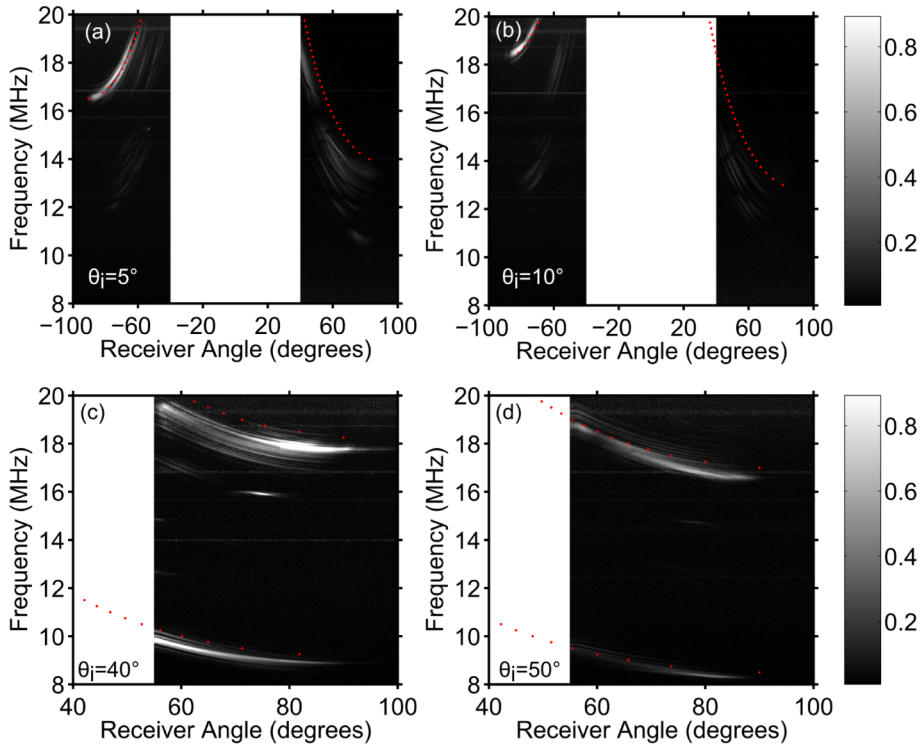

FIG. 5. Oblique incidence measurements for phononic crystal sample B ($h/a = 2$), obtained with the fixed emitter / rotated receiver setup. The red dotted line shows to the grating law (2). The incidence angle θ_i assumes the values (a) 5°, (b) 10°, (c) 40°, and (d) 50°.

C. Grazing angle receiver, rotated emitter

Figure 3 displays the measured angular spectrograms obtained with the fixed receiver / rotated emitter setup for both phononic crystal samples. The received spectra accumulate on discrete curves given by the grating law for diffraction. Indeed, from equation (2) for the grazing angle of diffraction ($\theta_n = -90°$), orders of diffraction are located on the curves

$$\omega = n\frac{2\pi c}{a}(1 + \sin\theta_i)^{-1}. \tag{5}$$

It can be seen that the corrugation depth influences the intensity of the diffracted wave. The first order diffracted intensity with the less deep phononic crystal (sample A) is more homogeneous than with the deep phononic crystal (sample B). Conversely, for angles of incidence around 0°, the diffraction efficiency is larger for sample B. Thus the diffracted intensity for a particular incident angle and frequency can be tuned by changing the corrugation depth. The most significant implication of the measurements, however, is that no grazing angle signal is recorded outside of the grating law. Hence, there is no apparent signature of surface waves.

D. Fixed emitter, rotated receiver

Figures 4 and 5 display the measured angular spectrograms for a series of fixed angles of incidence, and for samples A and B, respectively. The angle of incidence was given the arbitrary values $\theta_i = \pm 5°, \pm 10°, 40°$, and 50°. Because of mechanical mounts, there are missing angular ranges in the experimental data. It is found again that the diffracted spectra tend to accumulate mostly according to the grating law of equation (2). The diffraction efficiency is a rather slowly varying function of frequency and of the angle of incidence. The larger angles of incidence are seen to favor the diffracted efficiency. Though there is some energy that is detected away from the grating law curves, they could

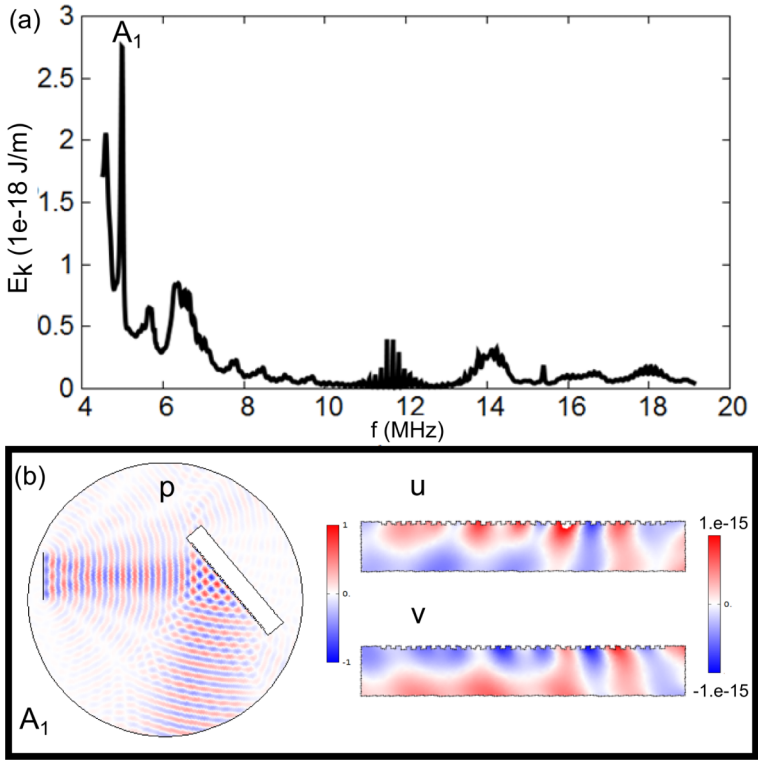

FIG. 6. Generation of elastic waves in the phononic crystal sample A ($h/a = 0.3$). (a) The elastic kinetic energy per unit length transferred to the solid from incident acoustic waves is plotted as a function of frequency. (b) Both the pressure distribution in water (left) and the displacements in the silicon grating (right) are shown for the solution of the time-harmonic acoustic-elastic coupled problem at the central frequency of peak A1 in (a). The angle of incidence is 40°. The computational domain is enclosed withing a circle along which a radiation boundary is applied. The time-harmonic finite element problem is solved as a function of frequency subject to a source of pressure waves placed in water and representing the emitting transducer.

not be clearly associated with surface wave signals. Significantly, no signal was detected below the diffraction cut-off frequency given by $\omega_1 = c/(2a) = 7.4$ MHz.

III. ANALYSIS

In order to gain insight in the diffraction process, we performed a time-harmonic finite element analysis of the diffraction of pressure acoustic waves on the one-dimensional phononic crystal gratings. The computation domain is two-dimensional, as the grating is homogeneous along the third dimension (see figures 6 and 7). A circle encloses it and is placed sufficiently far away from sources of waves. A radiation boundary condition is applied along the outer circular boundary so that reflections on it can be ignored in practice. The source of pressure wave is modeled by a line with prescribed unit pressure (1 Pa) oscillating at the acoustic frequency. The phononic crystal is modeled by a grooved silicon plate. Elastic waves inside the plate and acoustic waves in water are coupled by appropriate interface boundary conditions connecting the solid and fluid sub-domains.[10] The computation shown in figure 6 is obtained for the geometric parameters of sample A ($h/a = 0.3$) and an angle of incidence of 40°. In order to maintain numerical accuracy and to obtain a tractable problem size, the samples are represented by fewer grooves than in the actual experiment and the source width is also reduced. The plate thickness, however, remains to scale.

Figure 6(a) shows the total elastic kinetic energy per unit length that is stored in the silicon grating as a function of frequency. The idea is that if particular elastic waves are excited at some frequency inside the silicon grating, then we should be able to see some maximum in the diagram indicating that

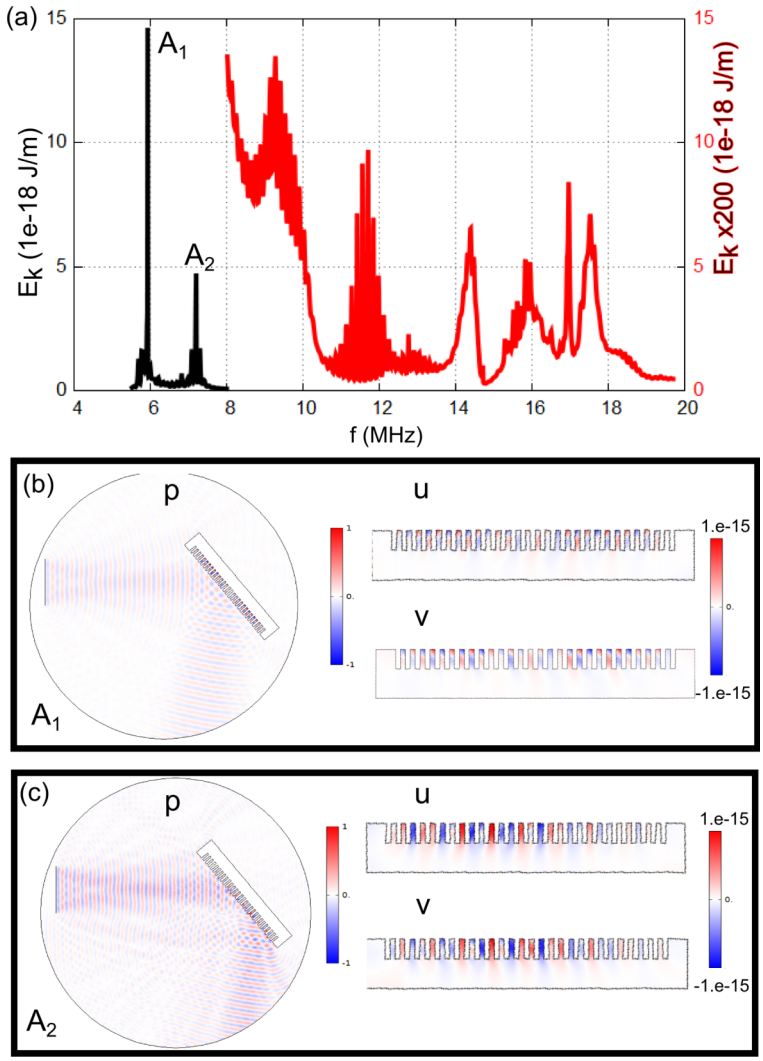

FIG. 7. Generation of elastic waves in the phononic crystal sample B ($h/a = 2$). (a) The elastic kinetic energy per unit length transferred to the solid from incident acoustic waves is plotted as a function of frequency. Note that two different energy scales are used to present the result; for frequencies above 8 MHz, the elastic kinetic energy has been multiplied by a factor 200 (red solid line) compared the values below 8 MHz (black solid line). (b,c) Both the pressure distribution in water (left) and the displacements in the silicon grating (right) are shown for the solution of the time-harmonic acoustic-elastic coupled problem at the central frequencies of peaks A1 and A2 in (a). The angle of incidence is 40°. The computational domain is enclosed withing a circle along which a radiation boundary is applied. The time-harmonic finite element problem is solved as a function of frequency subject to a source of pressure waves placed in water and representing the emitting transducer.

energy transfer from acoustic waves to elastic waves is actually taking place. In order to obtain this plot, the frequency is scanned from 4 to 20 MHz and the coupled acoustic-elastic problem is solved for every frequency. The kinetic energy spectrum indeed displays a series of resonances separated by frequency regions where little elastic energy is transferred to the grating by the incident acoustic wave. Figure 6(b) shows the wave field for the highest peak, appearing at a frequency of 5 MHz. This frequency is below the diffraction cut-off frequency ω_1, with the consequence that the generation of elastic waves at the peak frequency cannot be related to the phenomenon of diffraction of acoustic waves by the grating. The displacements fill all of the inside of the solid grating, resembling the distribution of a Lamb wave. The pressure wave reflected on the grating downward seems to be elongated along the interface, toward the right. We also plotted the wave fields for the other peaks in the kinetic energy spectrum, appearing at frequencies larger than ω_1, hence for which diffraction

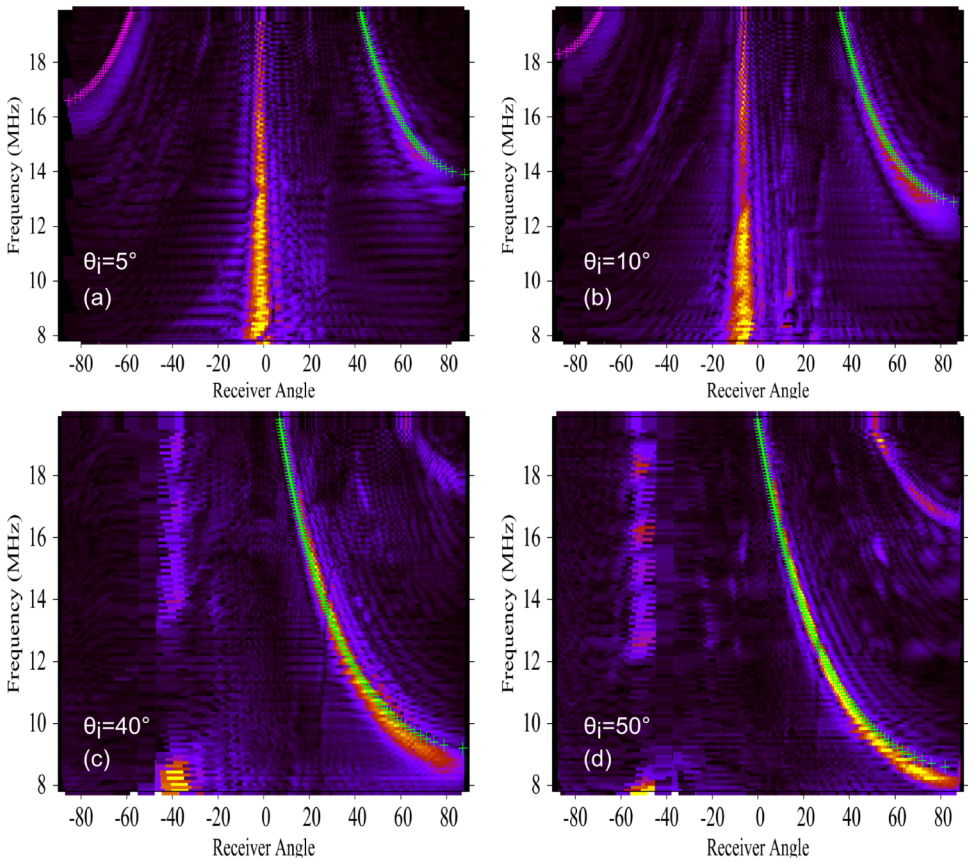

FIG. 8. Theoretical spectrograms obtained with FEM for phononic crystal sample A ($h/a = 0.3$). The angle of incidence is (a) 5°, (b) 10°, (c) 40°, and (d) 50°. The spectrograms are obtained from finite element computations similar to those shown in figures 6 a,d 7, by taking a 2D Fourier transform of the pressure distribution in water (see text for details).

occurs, but no beam displacement or extension effect could be observed in these cases. As a note, it is not possible to relate directly the frequency of the main peak at the frequency of 5 MHz to the dispersion relation of an interface wave propagating along the 1D phononic crystal grating as obtained in Ref. 10. The reason is that the dispersion relation for interface waves is obtained for an infinite grating, whereas the effect observed here is for a finite-extent acoustic beam. Furthermore, repeating the same calculation at other angles of incidence we would obtain a similar result as in figure 6, except for the peak frequencies changing slightly with the angle of incidence.

Figure 7 shows a similar computation for the deep grating corresponding to sample B ($h/a = 2$) and an angle of incidence of 40°. The transferred elastic kinetic energy is much stronger in this case, and there are two main peaks in the sub-diffraction frequency range. The wave fields for the first and the second peaks are shown in figures 7(b) and 7(c), respectively. The displacements are now mostly localized in the grooves and are evanescent in the substrate. The pressure in water is also maximal inside the groove trenches, indicating that there is a strong coupling occurring between acoustic and elastic waves. The pressure wave reflected on the grating downward undergoes a clear forward beam displacement effect at the second frequency, while the displacement is less marked at the first. It is also seen that the displacements within the grooves decrease fast as the surface elastic wave moves in the forward direction, indicating that it is strongly back-radiating acoustic energy into water. There are further much smaller peaks in figure 7(a) for frequencies above the diffraction cut-off frequency ω_1. The fact that these elastic resonances cannot be excited as efficiently as those below ω_1 is a further indication that surface waves have been excited.

As a final check, we verified that the finite element computation would give results in agreement with experiment. To this end, we computed wave-fields as a function of frequency for the different

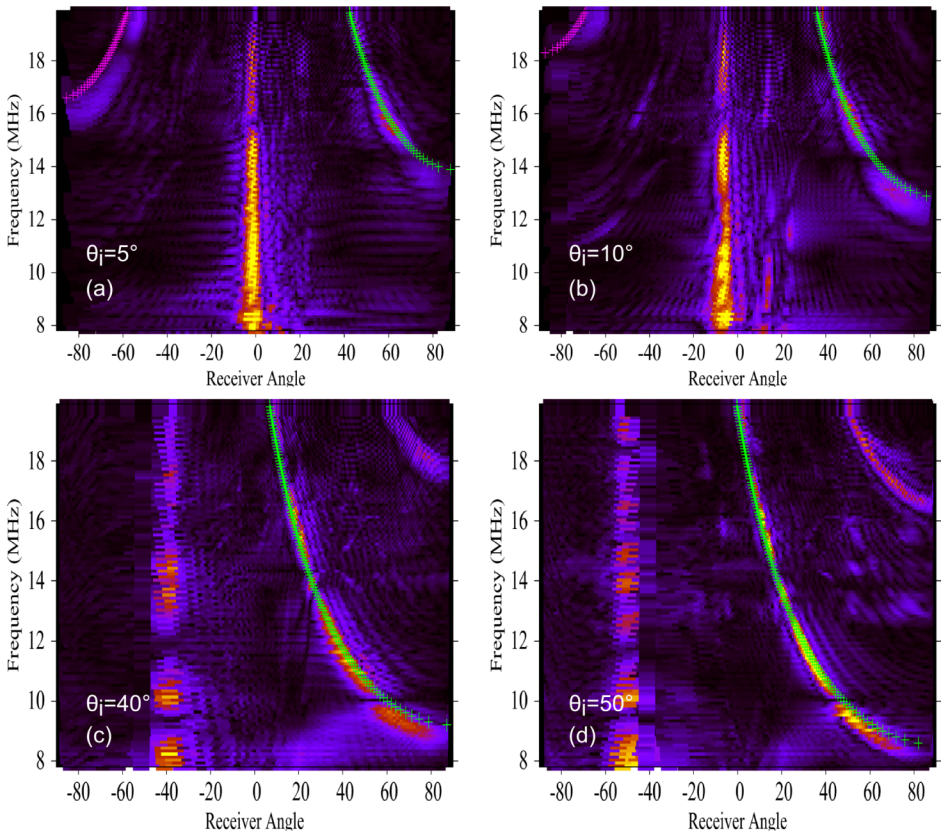

FIG. 9. Theoretical spectrograms obtained with FEM for phononic crystal sample B ($h/a = 2$). The angle of incidence is (a) 5°, (b) 10°, (c) 40°, and (d) 50°. The spectrograms are obtained from finite element computations similar to those shown in figures 6 a,d 7, by taking a 2D Fourier transform of the pressure distribution in water (see text for details).

incidence angles used in the experiments. For each wave-field, a 2D Fourier transform of the pressure distribution was taken. Since bulk waves in water satisfy the dispersion relation $\omega = ck$, they are expected to appear on a circle in k-space, with a radius given by the slowness $s = 1/c = 6.7\ 10^{-4}$ s/m. Gathering the result as a function of the emission angle, we could plot the theoretical spectrograms displayed in figures 8 and 9 for samples A and B, respectively. The numerical results compare favorably with the experimental results in figures 4 and 5. They confirm that waves in water distribute into the set available of diffraction orders and do not show any clear sign that surface wave generation has occurred. In view of applications as diffraction gratings to steer an incident acoustic beam into a diffraction order, both phononic crystal samples should clearly be used with a large incidence angle in order to maximize the diffraction efficiency.

IV. CONCLUSION

We have studied surface wave generation on deeply corrugated one-dimensional phononic crystal gratings by diffraction of acoustic pressure waves incident from water. In the experiments we could vary both the angle of incidence and the receiver position, hence catching most relevant information about waves propagating in water and originating from the grating. It is known from phononic crystal theory that since the dispersion relation of true surface waves of the grating lies below the sound cone in water and must respect periodicity, they can not be excited from the diffraction of infinite plane waves incident from water. Diffraction measurements with medium and deeply corrugated one-dimensional phononic crystals defined by etching in a silicon wafer indeed confirm that all propagating waves detected in water follow the grating law for bulk acoustic waves. It is found

that the diffraction efficiency to the first and the second diffraction orders is quite high over a wide range of incidence and frequency conditions. The transduction of surface guided waves on the grating, however, is not apparent from these measurements. Nevertheless, numerical simulations reveal that for frequencies in the sub-diffraction regime, the acoustic energy of a beam of finite extent can still be transferred to elastic waves propagating at the surface of the grating. These surface waves back-radiate acoustic waves in the specular direction and thus decay very fast as they propagate along the grating surface, a mechanism that explains the beam displacement effect, here identified in the forward direction. The obtained results could be applied to the design of novel transducers based on the conversion of bulk pressure waves into surface elastic waves, though moderate conversion efficiencies have been obtained with the considered samples.

ACKNOWLEDGMENT

Financial support by the Agence Nationale de la Recherche under grant ANR-09-BLANC-0167-01 is gratefully acknowledged.

[1] T.-T. Wu, L.-C. Wu, and Z.-G. Huang, J. Appl. Phys. **97**, 094916 (2005).
[2] S. Benchabane, L. Robert, J.-Y. Rauch, A. Khelif, and V. Laude, Phys. Rev. E **73**, 065601(R) (2006).
[3] I. El-Kady, R. H. Olsson, and J. G. Fleming, Appl. Phys. Lett. **92**, 233504 (2008).
[4] S. Mohammadi, A. Eftekhar, W. Hunt, and A. Adibi, Appl. Phys. Lett. **94**, 104301 (2009).
[5] S. Benchabane, O. Gaiffe, G. Ulliac, R. Salut, Y. Achaoui, and V. Laude, Appl. Phys. Lett. **98**, 171908 (2011).
[6] Y. Achaoui, A. Khelif, S. Benchabane, V. Laude, and B. Aoubiza, Phys. Rev. B **83**, 104201 (2011).
[7] H. Estrada, A. Uris, and F. Meseguer, Appl. Phys. Lett. **101**, 104103 (2012).
[8] H. Jia, M. Ke, C. Li, C. Qiu, and Z. Liu, Appl. Phys. Lett. **102**, 153508 (2013).
[9] H. Estrada, P. Candelas, F. Belmar, A. Uris, F. J. García de Abajo, and F. Meseguer, Phys. Rev. B **85**, 174301 (2012).
[10] R. P. Moiseyenko, N. F. Declercq, and V. Laude, J. Phys. D: Appl. Phys. **46**, 365305 (2013).
[11] V. G. Gogoladze, Trudy Seismolog. Inst. Acad. Nauk SSSR **127**, 27 (1948).
[12] J. G. Scholte, Nederl. Akad. Wetensch., Proc. **52**, 652 (1949).
[13] C. Desmet, V. Gusev, W. Lauriks, C. Glorieux, and J. Thoen, Appl. Phys. Lett. **68**, 2939 (1996).
[14] C. Glorieux, K. V. de Rostyne, K. Nelson, W. Gao, W. Lauriks, and J. Thoen, J. Acoust. Soc. Am. **110**, 1299 (2001).
[15] C. Glorieux, K. V. de Rostyne, J. Goossens, G. Shkerdin, W. Lauriks, and K. A. Nelson, J. Appl. Phys. **99**, 013511 (2006).
[16] R. P. Moiseyenko, S. Herbison, N. F. Declercq, and V. Laude, J. Appl. Phys. **111**, 034907 (2012).
[17] R. P. Moiseyenko, J. Liu, N. F. Declercq, and V. Laude, Appl. Phys. Lett. **102**, 034108 (2013).
[18] A. G. Every, R. E. Vines, and J. P. Wolfe, Phys. Rev. B **60**, 11755 (1999).
[19] T. Tamir and H. L. Bertoni, J. Opt. Soc. Am. **61**, 1397 (1971).
[20] M. A. Breazeale and M. A. Torbett, Appl. Phys. Lett. **29**, 456 (1976).
[21] X. Yin, L. Hesselink, Z. Liu, N. Fang, and X. Zhang, Appl. Phys. Lett. **85**, 372 (2004).
[22] X. Liu, Z. Cao, P. Zhu, Q. Shen, and X. Liu, Phys. Rev. E **73**, 056617 (2006).
[23] A. Teklu, M. A. Breazeale, N. F. Declercq, R. D. Hasse, and M. S. McPherson, J. Appl. Phys. **97**, 084904 (2005).
[24] N. F. Declercq, J. Degrieck, R. Briers, and O. Leroy, J. Acoust. Soc. Am. **112**, 2414 (2002).
[25] N. F. Declercq, J. Degrieck, R. Briers, and O. Leroy, J. Appl. Phys. **96**, 6869 (2004).
[26] N. F. Declercq, J. Degrieck, and O. Leroy, Appl. Phys. Lett. **85**, 4234 (2004).